Cement and Concrete Composites 90 (2018) 1–13

Contents lists available at ScienceDirect

Cement and Concrete Composites

journal homepage: www.elsevier.com/locate/cemconcomp

A self-reinforced cementitious composite for building-scale 3D printing

Daniel G. Soltan [a], Victor C. Li [a, b, c, *]

[a] Macromolecular Science and Engineering, University of Michigan, 2800 Plymouth Road, Rm. 3006E Building 28 NCRC, Ann Arbor, MI, 48109, USA
[b] Civil and Environmental Engineering, University of Michigan, 2350 Hayward Ave., Ann Arbor, MI, 48109, USA
[c] Materials Science and Engineering, University of Michigan, 2300 Hayward Ave., Ann Arbor, MI, 48109, USA

ARTICLE INFO

Article history:
Received 15 June 2017
Received in revised form
12 February 2018
Accepted 19 March 2018
Available online 20 March 2018

Keywords:
Printable concrete
Printable ECC
Strain-hardening cementitious composites
Three dimensional printing
Additive manufacturing

ABSTRACT

A design scheme for self-reinforced cementitious composites to be used for building-scale 3D printing processes is introduced. The design is based on that of engineered cementitious composites, which include dispersed short polymer fibers to generate robust tensile strain-hardening. The mechanical property profile of these printable ECC materials is meant to eliminate the need for steel reinforcement in printed structures, providing more freedom and efficiency for building-scale 3D printing processes. The fresh state rheological properties have been systematically manipulated to allow printability. Effects on fresh state workability of several compositional ingredients and processing parameters are investigated herein. To maintain consistent printing performance with a batch mixing approach, thixotropy in the fresh state is exploited to temporarily decouple hardening behavior from the processing timeline. Minimal workability loss under continued shear agitation is achieved. Mechanical properties of the printable materials are characterized and the printability of the materials is demonstrated.

1. Introduction

The modern construction industry has recently seen a push toward increased automation, led by recent advances in building-scale additive manufacturing processes [1–6]. The potential benefits of automated additive manufacturing processes for the construction industry have been previously enumerated and include improved efficiency and safety [5–10].

Three dimensional-printing of concrete has generated significant publicity and is the most widely recognized and applied method of additive manufacturing for construction applications. Many of the recent innovations in the area, in both academic and commercial research and development, have focused primarily on the equipment with which 3D concrete printing is conducted to improve the capabilities of the process.

Much less attention has been paid to the materials used for building-scale 3D printing, though this has also been studied [11–13]. While many engineering challenges related to the "printability" of the concrete materials used for building-scale 3D printing have been overcome, much of this work ignores the inherent weaknesses of traditional concrete and the implications of these weaknesses for 3D printed structures.

Traditional concrete is brittle and weak in tension, prone to failure in many common loading situations such as those that introduce bending moments or shear forces. For this reason, steel reinforcement is typically used to carry tension within concrete, and printed concrete is no exception. Steel reinforcement is susceptible to corrosion, which introduces additional tensile forces on the concrete cover and often leads to rapid deterioration of concrete structures. Additionally, the placement of steel reinforcement into a 3D printed structure is antithetical to the speed, ease, and design freedom promised by the freeform, bottom-up 3D printing paradigm. The need for placement of additional reinforcement in large 3D printed structures has limited the benefits, short of its potential, that the process has been able offer the industry.

In this study, a self-reinforced printable cementitious composite, designed to reduce or eliminate the need for steel reinforcement in printed structures, is introduced. A general design philosophy for printable cementitious materials, leveraging thixotropy, is described. Compositional ingredients and material processing parameters are investigated for their contribution to material behaviors that promote printability in cementitious materials.

* Corresponding author. Civil and Envirionmental Engineering, University of Michigan, 2350 Hayward Ave., Ann Arbor, MI, 48019, USA.
E-mail address: dsoltan@umich.edu (V.C. Li).

https://doi.org/10.1016/j.cemconcomp.2018.03.017
0958-9465/

Abbreviations

ANC	Attapulgite Nanoclay
CA	Calcium Aluminate Cement
ECC	Engineered Cementitious Composites
GS	Ground Silica
HPMC	Hydroxypropylmethylcellulose
MS	Microsilica

1.1. Printability

The material behaviors that define printability, the capacity for a material to be successfully processed via the 3D printing process, have been previously described for cementitious materials [1,10,11]. Lim et al. (2012) stated, "the wet properties of the [cementitious] material are critical to the success of manufacture", and go on to identify the key attributes of printability [1]. These attributes are (1) extrudability, the capacity of the cementitious material in the fresh (uncured) state to pass or be pumped through small pipes/nozzles and ultimately be deposited in an even, continuous filament, (2) buildability, the ability of a printed filament to hold its shape, particularly under the weight of subsequently printed layers, and (3) interlayer bonding, the ability of adjacent filaments to form a cohesive bond, producing a unified, structurally sound printed part. The authors of this paper would like to also stress that a truly printable heterogeneous composite material, such as concrete, will not suffer constituent segregation processing. This is to say that a printable cementitious composite should maintain a "uniformly heterogenous" structure while being deposited in the 3D printing process. Each of these parameters (extrudability, buildability, interlayer bonding, and segregation prevention) is dependent on "workability", a descriptor of the rheological properties of a freshly mixed cementitious material. Workability can be equated to "flowability", an often-used metric to indirectly, but quantitatively, evaluate the rheology of freshly mixed cementitious materials.

Extrudability and buildability are competing factors in that high workability promotes extrudability, while low workability promotes buildability. Additionally, low workability can negatively affect interlayer bonding, and excessively high flowability can, in some cases, cause segregation of constituents. These key attributes—extrudability, buildability, interlayer bonding, and segregation prevention—must be properly balanced to allow printability.

"Open time" is defined as the period of time in which the workability is consistent within certain tolerance acceptable for 3D printing. This is the interval of time over which the material is actually "printable". In this work, we aim to design a "printable" material that can be processed with the batch mixing approach, as opposed to continuous mixing, as batch mixing is much more broadly feasible and widely applied in practice. Thus, designing for batch processing will lead to more rapid and meaningful research outcomes. This does, however, add a challenging timing variable to the "printability" equation. Because the material is mixed and prepared for printing in large batches, and because not all the material will be printed simultaneously, there will be a variable time between when a specific unit volume of material is hydrated and when that same unit volume is deposited by the printer head. This challenge is explained and addressed in Section 1.3.

1.2. Thixotropy and minimal workability loss for printability

An idealized behavior of a "printable" cementitious material as described above is summarized in terms of flowability over time, or "flowability evolution", in Fig. 1. Between the time the material is thoroughly and completely mixed, $t = 0$, and the time the material is printed, $t = T_p$, the material should be "extrudable" which corresponds to a large range of flowability values above a certain critical value, but not so flowable as to allow segregation of constituents. At the time the material is deposited by the printer head, the material needs to be both extrudable and immediately buildable, corresponding to another range of flowability values below that certain critical value. The material needs to first hold its shape when extruded in a predictable way, and by the time subsequent layers are deposited upon it, be able to support those respective weights without excessive deformation. The ideal material should be flowable prior to deposition, be both extrudable and buildable at the time of deposition, and rapidly harden after deposition.

Because the time from mixing to being deposited (due to the batch processing typically used for cementitious material) would not realistically be constant for a large-scale print, the time at which the material rapidly hardens needs to be decoupled from the time the material is mixed, or more precisely, the time from which the material is hydrated. A graphical representation of this theoretical behavior subject to the constraints of construction and cementitious material processing is presented in Fig. 2.

As Fig. 2 indicates, there should be minimal workability loss (corresponding to change in flowability, ΔF_f) between the start of deposition to end of deposition. In practice, minimal workability loss during deposition can be extrapolated to also require a low decrease in flowability between the end of mixing to the end of deposition. This "harden on command" flowability evolution is atypical and challenging for typical cementitious materials.

Thixotropic rheological behavior can theoretically be exploited to generate this flowability evolution behavior in which hardening is decoupled, at least temporarily, from time after mixing [14]. Thixotropic materials can be described as having a reduced viscosity (i.e. increased flowability) when a shear stress, such as stirring, is applied, compared to the unperturbed state. Viscosity is regained in a thixotropic material when the applied shear stress is removed, in a process called rebuilding. In a 3D concrete printing system, shear stresses are applied in the pumping process. Additional agitation can be performed as needed in the material feeding system. A cementitious material that is thixotropic with rapid rebuilding, as illustrated graphically in Fig. 3, could therefore be highly printable.

A range of flowability values in which the material is both extrudable and buildable, as indicated in Fig. 3, would also be advantageous. Thixotropy would allow a range of flowabilities in which the material is simultaneously extrudable when a shear stress is applied, and buildable when that shear stress is removed.

To guide the design of printable cementitious materials, this study investigates (1) the effect of several compositional ingredients reported to promote thixotropic and anti-segregation behaviors in mixtures on the attributes associated with printability of cementitious composites (flowability and hardening behavior), and (2) relevant processing parameters having effects on the same. There is no singular requirement directed to the open time and hardening time of cementitious materials for building-scale printing, so the materials formulated and developed in this work are instead designed to have tunable rheological and hardening behavior such that hardware-specific development can be done efficiently and systematically. The "flowability evolution" results presented herein for specific ingredients, dosages, and processing parameters are meant to show the mechanisms through which rheology and hardening behavior can be tuned for any given hardware. What is meant to be demonstrated is hardware agnostic printability via thixotropic behavior (specifically minimal workability loss and rapid rebuilding), in combination with mechanical

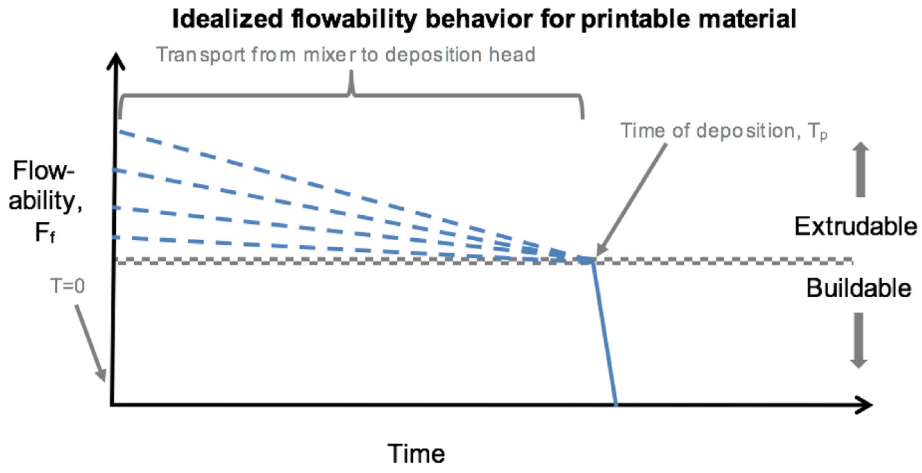

Fig. 1. The idealized flowability behavior for a cementitious printable material is graphically represented in terms of flowability evolution, wherein the material is extrudable prior to deposition, extrudable and buildable at the time of deposition, and rapidly hardening after deposition so as to become increasingly buildable. The loss of flowability prior to deposition could theoretically take place at any rate, as long as deposition occurs when the material is both extrudable and buildable.

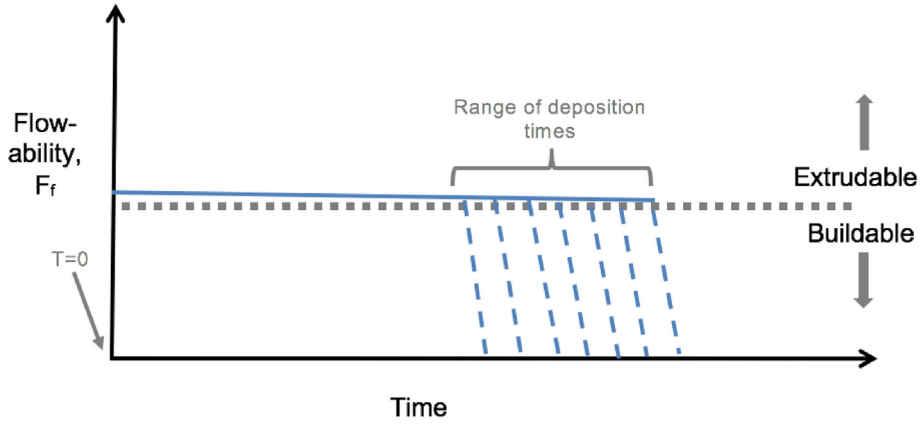

Fig. 2. The theoretical flowability evolution required for consistent 3D printing, given common practical constraints of construction and cementitious material processing.

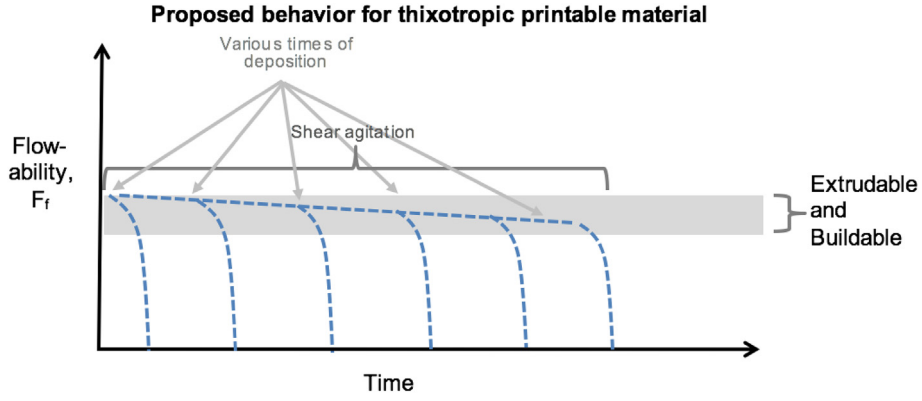

Fig. 3. Proposed flowability evolution for a realistically printable cementitious material derived via thixotropy and rapid rebuilding.

behaviors that promote durability in cementitious materials.

1.3. ECCs as durable materials for building-scale 3D printing

Engineered cementitious composites, a family of cementitious materials compatible with typical concrete processing methods and exhibiting strain-hardening behavior by way of a low volume fraction amount of dispersed polymer fibers, have been developed for the purpose of improving the durability and resiliency of critical structural and infrastructural components. The micromechanics of ECCs have been previously described, and differ from those of other fiber reinforced concretes [15]. In short, when the brittle cementitious matrix fractures in tension, the dispersed fibers are able to bridge the crack, holding the crack to several tens of microns in

width, while carrying the tensile load such that further opening of the microcrack requires more energy than originating a microcrack elsewhere in the matrix. This cycle can be repeated many times, such that the composite is able to distribute deformation throughout and suppress brittle fracture failure. ECCs are more damage and flaw tolerant than other fiber-reinforced materials because strain-hardening behavior, rather than strain-softening behavior, is generated. In fact, ECCs exhibit tensile ductility (strain capacity prior to failure, where failure is defined as the inability to carry and increasing load) and toughness (energy required to cause failure) hundreds of times those values of traditional concretes, providing the potential to eliminate or diminish the amount of steel reinforcement necessary to accommodate tensile loading.

Engineered cementitious composite materials have been previously developed for the casting application method typical of concretes [16], as well as the spraying method typical of "shotcretes" [17,18]. In this study, a material exhibiting the characteristic strain-hardening behavior of ECCs is designed to have the distinct rheological properties required for functional compatibility with building-scale 3D printing processes (i.e. printability).

While fiber reinforcement in printable cementitious materials has been studied in the past [11–13], the fibers in these cases are generally included to mitigate the effects of drying shrinkage and do not promote robust tensile strain hardening behavior, which is responsible for the load-carrying capacity and durability of ECCs, in the printable material.

2. Materials and methods

2.1. Evaluation of fresh state properties

Fresh state workability has been identified as being crucial to the printability of cementitious materials. In this study, the fresh state is defined as the condition of the complete composite composition (including dispersed fibers) in the short time period after complete mixing has been concluded, and in which printing would theoretically take place. In this work, workability is quantitatively assessed using the flowability factor, measured via the drop table test (ASTM C1437 and ASTM C230), as used previously for investigations of thixotropic [19] and printable [10] cementitious materials. In the present study, the flowability factor of cementitious pastes (completely mixed compositions, including fibers) is measured over time (after mixing is stopped) to generate a "flowability evolution" curve, providing a convenient method of describing the change in workability (stiffening) over time intervals relevant to 3D printing. The simplicity of this method of assessing workability over time allows it to be used (1) to accelerate the design process of new printable mixes and (2) as a realistic, on-site quality control technique.

2.2. Compositional ingredients

The material compositions investigated in this study are inspired by previously reported engineered cementitious composites. Several compositional ingredients, listed in Table 1, are included due to their reported effects on the fresh state and early stage properties, hypothesized to promote target behaviors for printable cementitious materials.

Composition is used as variable throughout the study and compositional variations in the reported results are labeled accordingly. Several important mix compositions reported herein are described and labeled in Table 2. All compositional components are reported in percentage, by weight, of the total cementitious material. In this study, "total cementitious material" is defined as (Type I cement + Fly Ash + calcium aluminate cement) by weight. All mixes contain 2% by volume polyvinylalcohol (PVA) fiber cut to 12 mm, the typical fiber volume fraction for ECC materials. Fiber is included in all the mixes for all tests due to its significant effect on properties in both the fresh and cured states.

Additional information about each of the compositional ingredients can be found in Appendix I.

2.3. Mix processing

Mixing of the cementitious compositions is conducted in KitchenAid (6 qt.) or Hobart (12 gal.) planetary-style mixers. Because the mixing process, including the order of ingredient addition and time of addition, affect the fresh properties of the cementitious paste, this procedure was conducted according to an explicit schedule. Dry ingredients (excluding ANC, HPMC, and MS) are mixed first for at least 5 min. A portion of the water content is added at time zero, followed by the high range water reducing agent (HRWRA) at $t = 30$ s, and the MS content between $t = 1{:}00$ min and $t = 2{:}00$ min.

Remaining portion of the water content is mixed with the ANC and used for the ANC exfoliation process, similar to that described in Kawashima (2013), in a standard 40 oz./700 W blender [24,25]. The portion of the water content separated out for this process is ~0.7–1.0 L, depending on the batch size, sufficient to cover the blender blades and for rinsing of the blender jar to ensure nearly all of the exfoliated ANC content is added to the mix. The ANC is exfoliated in water (blended) for at least 3 min before being added to the mix. The ANC content, and associated water content, is added to the mix at $t = 6$ min. For mixes not including ANC, the entirety of the water content is added at time zero.

Half the HPMC content is added at $t = 8$ min, followed by the addition of fibers in small handfuls between $t = 9$ min and $t = 12$ min, after which the remainder of the HPMC content is added. Mixing continues until $t = 28$ to ensure even dispersion and activation of the viscosity modifying ingredients.

In addition to compositional ingredients, several processing parameters were investigated for their effect on fresh state properties. Water temperature and batch size, two controllable processing parameters, were used as variables. The water content for each mix reported herein, unless otherwise stated, can be assumed to be 20–25 °C at time of addition. Three typical batch sizes are used in this study: 1.2 L, 3.1 L, and 6.2 L, which will hereafter be referred to as small, medium, and large batches.

2.4. Workability loss evaluation method

For the investigation of workability loss, half of the mix volume is removed from the mixer at $t = 28$ min, and drop table flowability testing is performed at regular time intervals. The other half of the mix volume remains in the mixer and continues to be mixed for an additional 15 min and is removed at $t = 43$ min, at which time flowability testing is performed. Comparison of the flowability evolution between these two volumes of the same mix determines the workability loss with continued agitation. Minimal workability loss is targeted for robust printability.

While thixotropy is not directly measured via hysteresis in this study, workability loss is used as an indicator of "single cycle" thixotropy over the short time scale in which a cementitious material would be printed.

2.5. Printability evaluation methods

A manual extrusion technique was used as a preliminary, small-scale approximation of the final step of typical 3D printing

Table 1
Ingredients investigated for utility in printable cementitious compositions.

Ingredient	Reported Effects in Cementitious Pastes
Calcium Aluminate Cement (CA)	*Early flowability followed by rapid hardening, high early strength* [10,17]
Hydroxypropyl Methylcellulose (HPMC)	*Increased viscosity, segregation prevention during pumping, and thixotropy* [17,21]
Microsilica (MS) and ground silica flour	*Early strength and thixotropy* [22,23]
Attapulgite Nanoclay (ANC)	*Thixotropy and enhanced cohesion* [19,24,25]

processes designed for concrete. This printing approximation technique used a mechanically actuated caulk gun, pictured in Fig. 4, with circular nozzle diameters 8 mm–13 mm. In lieu of a progressive cavity pump, a peristaltic pump with a 3 cm tube diameter and 4 cm × 1.5 cm flat tip nozzle was used for a large scale approximation. Manual agitation of the material in the hopper of the peristaltic pump was performed to maintain adequate workability over the period of printing.

2.6. Mechanical performance evaluation methods

Uniaxial tensile and compression testing was used to evaluate mechanical performance of the materials. Tensile specimens were prepared via casting using dogbone [26] and coupon conformations, as well as via the manual printing approximation technique in the coupon shape. Both casting and the manual printing approximation technique were used to produce cubic specimens for compression testing (the "printed" cube speciemens were sectioned after curing to attain flat faces and standard dimensions). All test specimens were cured in air at room temperature as would be realistic for printed forms in practice. Mechanical testing on the composites was performed 28 days after being mixed and formed.

Tensile testing was performed with a universal tensile testing machine (Instron), with constant displacement loading at a rate of 0.005 mm/s, based on the recommendations of the JSCE [26]. Ultimate tensile strength is reported herein as the stress at the maximum load sustained by each composite. Strain capacity is reported as the strain at maximum stress carried by the composite prior to terminal stress decay.

Compression testing was performed with a Forney compression machine with cube-shaped specimens. Compression testing specimens produced via the manual printing approximation were "printed" in a near cubic or rectangular prism three-dimensional shape, then sectioned after curing to standard cubic dimensions. A loading rate of ~50 psi/s was used, based on recommendations of the ASTM C109 International standard. Compressive strength is reported as the stress at the maximum load sustained by the composite.

3. Results and discussion

The flowability evolution of typical ECCs (represented by Mix 0), designed for casting, is not appropriate for 3D printing due to high initial flowability and the long time required for the material to harden, as illustrated in Fig. 5. For comparison, Mix 1 is also plotted in Fig. 5. In Mix 1, HPMC was used as a thickening agent to create a mix that exhibited flowability values that allowed extrudability and the ability of the extruded filament to hold its shape. Preliminary testing, using the manual extrusion approximation technique, showed that flowability factor values between 1.4 and 1.2 were an appropriate target for extrudability and shape stability under self-weight, however rapid hardening is also required for buildability. Mix 1 shows that manipulation of viscosity via HPMC and cement/

Table 2
Several key mix compositions are described. All compositions are reported in percentage of total cementitious material (%C.M.), apart from fiber content which is reported in volume fraction.

	Type I Portland Cement	Class F Fly Ash	Calcium Aluminate Cement	F-75 Silica Sand	MS	GS	Water	ANC	HPMC	HRWRA	PVA Fiber (% by vol.)
Mix 0	45.5	54.5	0.0	36.3	0.0	0.0	26.4	0.0	0.0	0.3	2.0
Mix 1	76.9	23.1	0.0	61.5	0.0	0.0	35.4	0.0	0.4	0.6	2.0
Mix 2	76.9	23.1	0.0	61.5	0.0	0.0	38.0	0.0	0.4	0.8	2.0
Mix 3	69.6	22.4	8.0	60.0	0.0	0.0	37.2	0.0	0.4	0.8	2.0
Mix 4	69.6	22.4	8.0	45.0	10.0	5.0	43.0	0.0	0.4	0.8	2.0
Mix 5	72.0	23.0	5.0	45.0	10.0	5.0	43.0	0.5	0.4	0.8	2.0
MS:	microsilica				**GS:**	ground silica					
ANC:	attapulgite nanoclay				**HPMC:**	hydroxypropylmethylcellulose					
HRWRA:	high range water reducing agent				**PVA:**	polyvinylalcohol fiber (12 mm)					

Fig. 4. A mechanically actuated, manually operated caulk-gun apparatus, shown with a pencil for scale, was used as a means of extrusion for a small-scale approximation of the final step of the 3D printing process. Nozzle diameters 8–13 mm were used.

fly ash ratio is successful in modifying the flowablity factor to fall within this range. However, a practical printable cementitious material is not achieved due its slow rate of hardening. Rapid hardening (after extrusion) is desired to accommodate the weight of many subsequently deposited layers and to facilitate time-efficient construction.

3.1. Compositional effects on workability evolution

3.1.1. Calcium aluminate cement

Calcium aluminate cement (CA) was seen to be effective in manipulating the rate of hardening. Mix 2 was used a baseline to illustrate the effect of CA dosage on the rate of hardening. Water content was adjusted slightly to allow sufficient mixing and fiber dispersion for several dosages. The effect on flowability evolution of various dosages of CA, in the small batch size, is illustrated in Fig. 6. The rapid hardening seen in CA/Portland cement mixes has been previously attributed to "the rapid formation of Ettringite and secondarily due to the hydration of CAC" [20]. In larger batch sizes, the rapid hardening rates seen in Fig. 6 for CA9+ were achieved with lower CA dosages (5% C.M.), with the addition of ANC and increased water temperature.

3.1.2. Microsilica and silica flour

Microsilica, substituted for silica sand by weight, was seen to increase the rate of hardening (Fig. 7), however significant increase in water content was required to produce proper dispersion of fiber, and effects of the increase in water dominated at the higher water contents. Though the higher water contents produced acceptable early flowability, they also produced longer time to hardening.

As seen in Fig. 7, introducing ground silica (GS), also called silica flour, in addition to MS was seen to allow both the early flowability and a rapid rate of hardening. This is likely due to a more even particle size distribution caused by the substitution of MS and GS for silica sand—the GS has an average particle size between those values of F-75 silica sand and MS. This promising composition incorporating both MS and GS is Mix 4.

3.1.3. Attapulgite nanoclay

The effect on workability evolution of ANC dosages is illustrated in Fig. 8. A thickening effect, reducing the flowability and time to hardening, is seen when mixed into large batch sizes. Rate of hardening ($\frac{\Delta F_f}{t}$) is slightly increased.

An effect on the mitigation of workability loss was also observed at the 0.5% C.M. and 0.8% C.M. dosages of ANC, as discussed in Section 3.5.

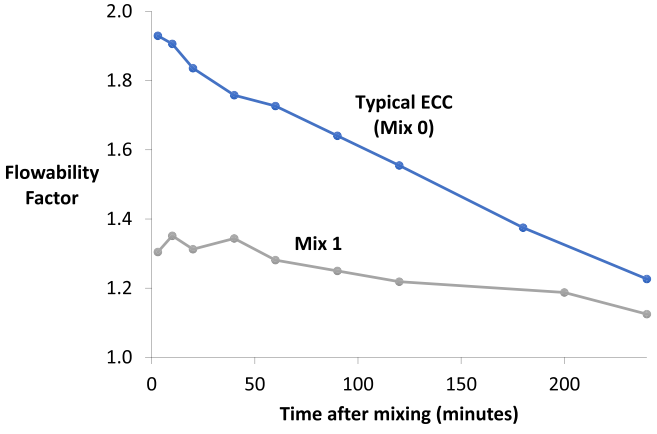

Fig. 5. The flowability evolutions for a typical castable ECC (Mix 0) and a viscosity modified version (Mix 1) incorporating HPMC. Neither flowability evolution is appropriate for 3D printing due to the long hardening times.

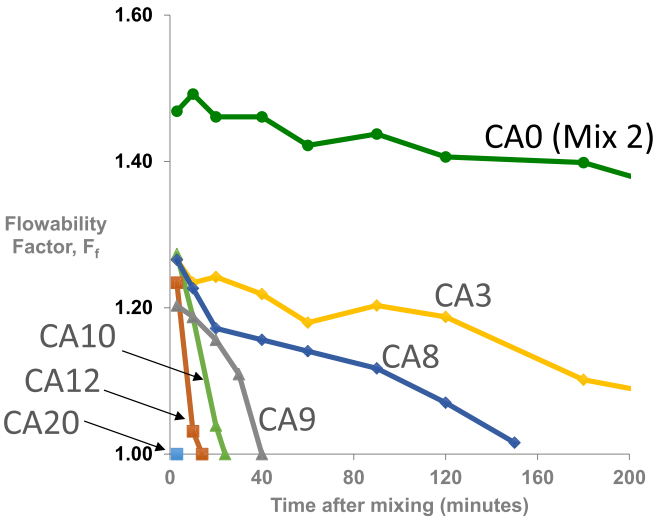

Fig. 6. Effect of calcium aluminate dosage on the flowability evolution of the cementitious composite in the small batch size, where CA0, CA3, and CA8 et cetera, represent calcium aluminate cement content of 0, 3, and 8 et cetera percent by weight of total cementitious material, respectively.

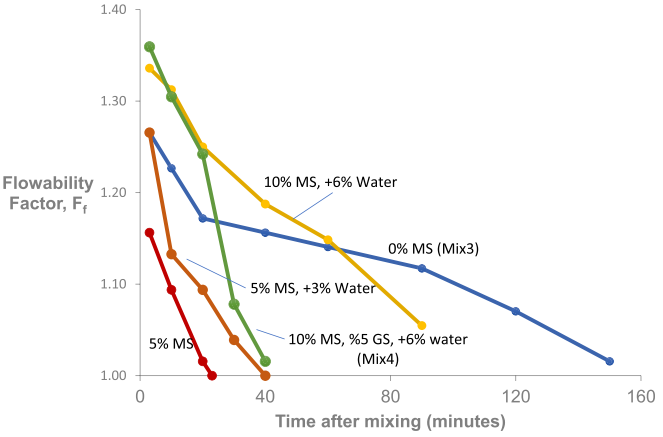

Fig. 7. The effect of microsilica (MS) dosage on flowability evolution in the small batch size. These mix compositions are based on Mix 3 and inspired Mix 4.

3.2. Water temperature effect on workability evolution

The Mix 4 composition was used to illustrate the effect of water temperature on workability in the fresh state, as seen in Fig. 9. The flowability evolution curves for the three clustered, intermediate temperatures illustrate the degree of variability to be expected between different batches of the same composition. Most current concrete printing technology hardware should be able to handle a degree of material variation for practical application, but it is recommended that water temperature be carefully monitored and controlled for mixing of printable cementitious composites. Water temperature can also be used to intentionally manipulate the fresh state properties of a particular mix composition. Water temperature affects fresh state rheological properties due to the accelerated activation of pozzolonic reactions of the cementitious materials.

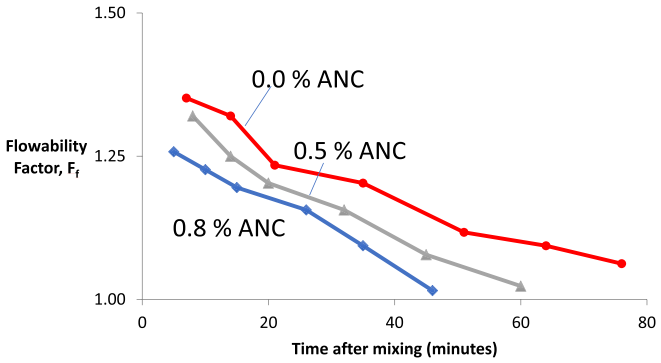

Fig. 8. ANC is seen to reduce flowability and reduce the time to hardening.

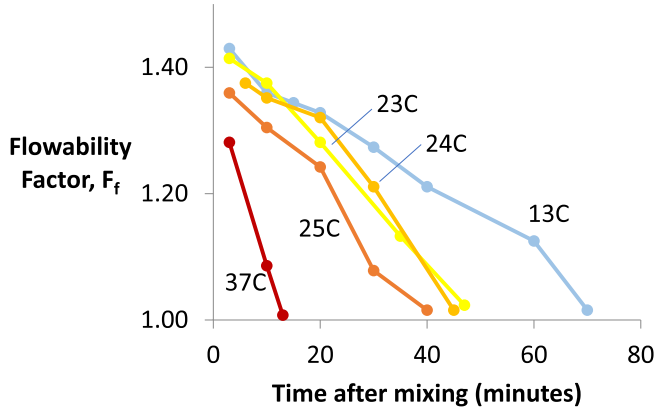

Fig. 9. Effect of water temperature on flowability evolution in Mix 4 (small batch).

3.3. Mechanical performance characterization

3.3.1. Performance in tension

Tensile performance of each composition was evaluated to confirm robust tensile strain hardening behavior. Mix 4 performed similarly to castable ECC compositions when each was tested in the cast form (Fig. 10). Specimens were tested in the cast dogbone form to determine the inherent tensile properties of the material itself. This specimen type generally measures the material's ideal tensile performance due to the shape of the specimen which encourages fiber alignment and mitigation of stress concentrations and flaws.

To assess the tensile performance in the printed or "structured" state, specimens were prepared with Mix 4, using the manual extrusion approximation technique described in Section 2.5. This technique allowed specimens to be produced with aligned filaments in multiple layers (see Fig. 11), mimicking the structure of a printed form. This form includes imperfections, such as rough, ribbed surfaces, and the joints (and sometimes small gaps) between adjacent filaments. These specimens were "printed" in the rectangular shape of the coupon specimens often used to test cast cementitious materials in tension.

As seen in Fig. 12, these "printed" coupon-shaped specimens, with filaments aligned along the loading axis, were compared under direct tension with "cast" specimens (coupon form) of the same composition (Mix 4), to illustrate the effect on mechanical performance of the structuring that would result from the 3D printing process. The average ultimate tensile strength and strain capacity of the printed and cast specimens are compared in Fig. 13. The superior performance in the printed form can be attributed to a much higher degree of fiber alignment in the tensile direction. Fibers preferentially align with the filament direction due to the restricted filament dimension and flow direction associated with the extrusion process.

The degree of fiber alignment is likely to be reduced as the filament size is increased for process scaling, but alignment is still expected to be generated based on the material flow/extrusion process. Deliberate nozzle design may be used to enhance fiber alignment even as the process is scaled. This control over fiber alignment (parallel to the 3D printing toolpath) will provide for opportunities to (1) reinforce critical areas of structures vulnerable to failures in tension, (2) impart mesoscale material structuring for functional grading or deformation mode manipulation, and (3) optimize mechanical properties for a given structure or part.

There may be a degree of matrix densification that occurs in each filament due to the squeezing action applied to the filament during the extrusion process, perhaps explaining the higher first cracking strength and ultimate tensile strength exhibited by the printed specimens in Fig. 12.

Multiple curves for each type of specimen are included in Fig. 12 to illustrate the range in performance observed for each type of specimen. The variable performance of the printed specimens can likely be attributed to the inhomogeneity of flaw size produced by the printing process and/or pattern. Regarding the difference in mechanical behavior when compared to the tensile performance of the dogbone specimens: the coupon specimen form generally approximates material performance in the bulk state, with minimal fiber alignment, such as how the material would be structured in a large-scale cast form.

3.3.2. Performance in compression

The effect on compressive strength of the printing process structure was also tested. Specimens printed in a cubic shape (with minimal intentional internal voids) were compared to specimens cast into the cubic shape. The results are compared in Fig. 14. No significant difference in compressive strength was observed.

Early strength of a printable composition is important due to the significant amount of weight it is expected to support in the hours after being deposited, as the otherwise unsupported member or structure is constructed. The early strength of the Mix 5 composition, containing ANC, was measured using compressive testing of cast cube specimens to ascertain material properties of the composition (Fig. 15). This Mix 5 composition is shown to meet all other requirements of a printable cementitious composite (extrudability, buildability, rapid hardening, and robust tensile properties). These compressive strength values are not necessarily representative of any particular printed member formed with this composition due to flaws that could arise from the printing process, but rather an accurate representation of the inherent material properties of the composition. These values are similar to those reported for printable concrete by Rushing et al. (30–38 MPa at seven days after mixing) [10]. It could be realistic to expect, due to the geometry of the printed filaments (high surface area), that strength may be gained even more quickly in a printed form.

3.3.3. Interlayer bonding characterization

The interlayer bond strength is another important aspect of the printed form of cementitious composites. To characterize the strength between adjacent printed filaments coupon tensile specimens were sectioned from the printed pattern pictured in Fig. 16. Specimens were printed and cured in the partially supported 45-degree angle arrangement pictured. Filaments were aligned normal to the axis of loading.

Four specimens of the Mix 4 composition were tested. The

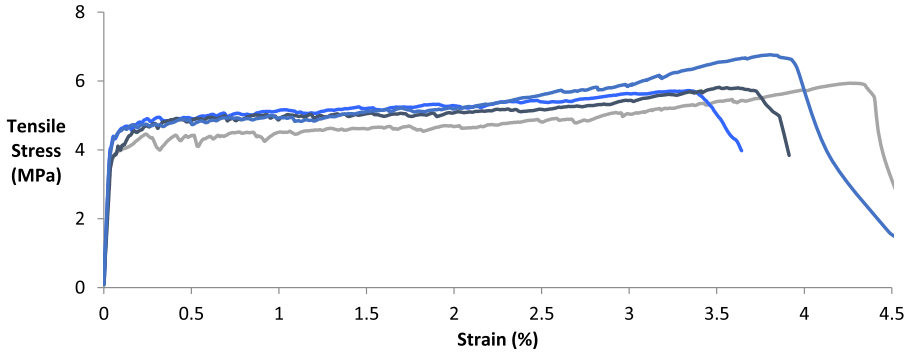

Fig. 10. Stress-strain curves (blue) of specimens cast with Mix 4, tested under direct tension, are compared with a representative curve (gray) for a typical ECC material (Mix 1), using dogbone shaped specimens. (For interpretation of the references to colour in this figure legend, the reader is referred to the Web version of this article.)

Fig. 11. "Printed" coupon specimens, including sectioned coupons mounted in the universal tensile testing instrument to show orientation.

average interlayer bond strength was measured to be 0.9 MPa with a standard deviation of 0.5 MPa. This is a conservative characterization of the average interlayer bond strength as it represents the weakest of the three bond lines in each tensile specimen. An example of a tested specimen is seen in Fig. 17. All specimens ultimately failed along one of the bond lines within the gage section, though all specimens showed a plurality of cracks, demonstrating a degree of failure suppression.

3.4. Batch recalibration for printable compositions

It was seen that batch size has an effect on the fresh state properties of the cementitious compositions reported here. Larger batch sizes generally showed higher flowability and slower rates of hardening than the same composition proportions mixed in the small batch size (1.2L), as illustrated for Mix 4 in Fig. 18.

A mix composition that mimicked the flowability evolution seen

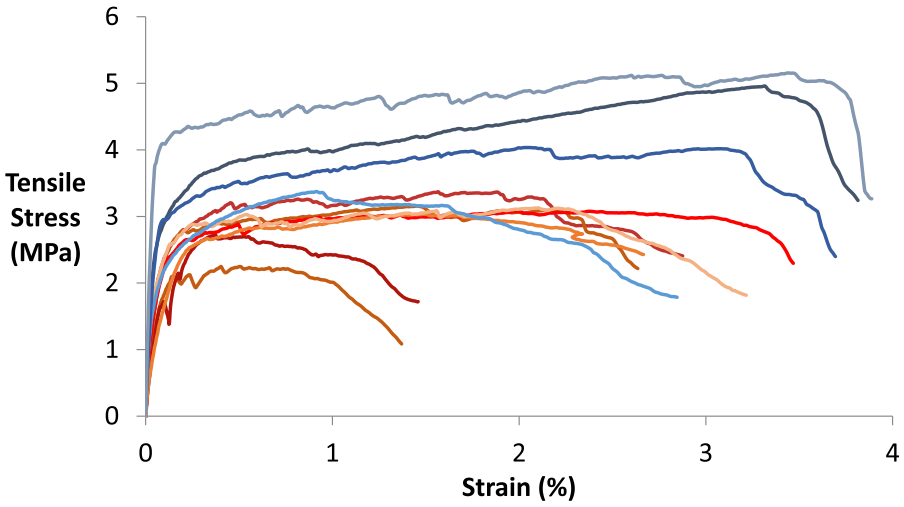

Fig. 12. The printed specimens (blue curves), with highly aligned fiber orientation, outperform the cast specimens (red curves) composed of the same material, when compared using the coupon specimen shape. (For interpretation of the references to colour in this figure legend, the reader is referred to the Web version of this article.)

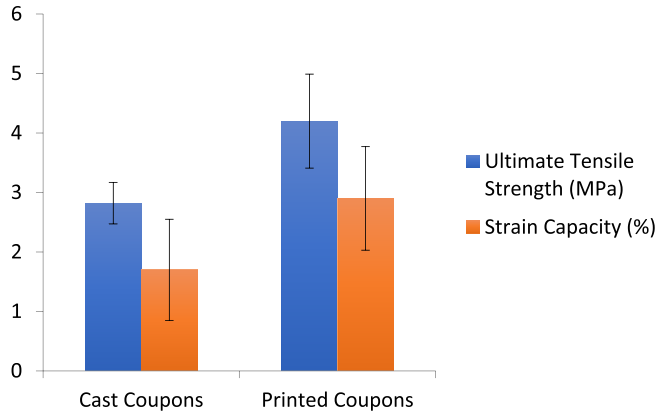

Fig. 13. The effect on tensile strength and strain capacity of the printed structuring is illustrated with the Mix 4 composition.

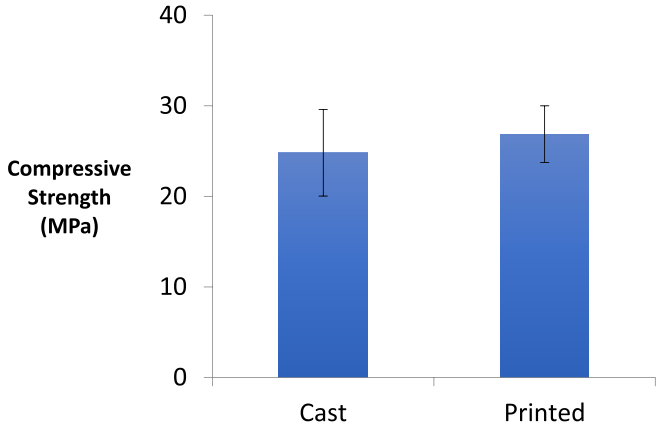

Fig. 14. No significant difference was seen in compressive strength between structures produced by the casting and printing processes, using the Mix 4 composition.

in the small batch version of Mix 4 in the medium batch size was derived by reducing the CA content, adding attapulgite nanoclay,

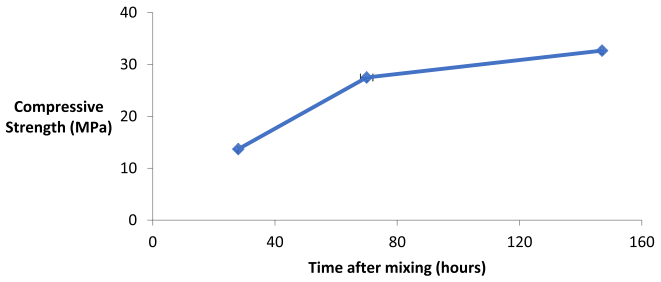

Fig. 15. Early strength of the Mix 5 printable ECC composition is measured over time.

and using a water content with an elevated temperature. The flowability evolution of this recalibrated composition (Mix 5) is compared to that of Mix 4, mixed in a small batch, in Fig. 19. CA content was reduced based on the results reported in Section 3.5, ANC was added based on results of Section 3.1 and 3.5, and the use of elevated water temp. was based on results reported in Section 3.2.

Batch size is a processing parameter that should be accounted for in scaling processing of printable cementitious materials. The results reported in Sections 3.1 and 3.2 can be used to guide material design.

3.5. Workability loss evaluation

Under the workability loss test scheme described in Section 2.4, Mix 4 exhibited significant workability loss. As seen in Fig. 20, with an additional 15 min of applied shear agitation (mixing), the fresh state material showed reduced flowability factor values at every time interval. Even if this (+15 min mixing) flowability curve is shifted 15 min on the x-axis (as represented by the dotted curve in Fig. 20) to account for the additional time spent in the mixer, the flowability factors are still less than those values at the same time intervals for the portion of the mix not subjected to additional mixing. This indicates that for this composition, continued shear agitation *accelerates* hardening and loss of workability, which is not desirable for consistent, controllable printing performance.

Attapulgite nanoclay and reduced CA content were seen to

Fig. 16. Preparation of the print pattern to be used in interlayer bonding testing of Mix 4 via the approximated 3D printing technique. Coupon shaped specimens were sectioned from the print pattern and tested in tension with the loading axis normal to the bond lines between filaments.

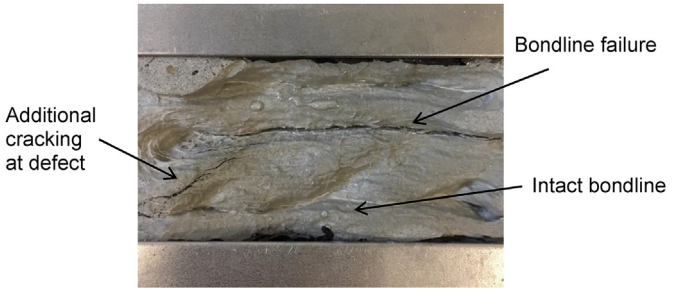

Fig. 17. An example of a tested interlayer bonding specimen.

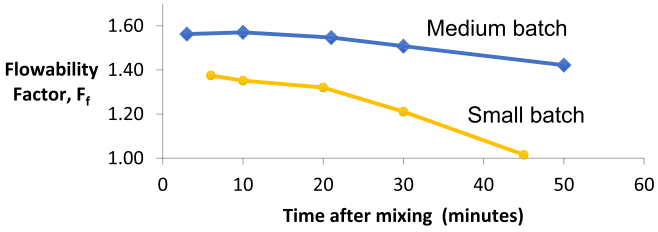

Fig. 18. Comparison of flowability evolution for Mix 4 mixed in small (1.2 L) and medium (3.1 L) batches. The flowability evolution associated with the small batch here is considered more appropriate for use with the 3D printing process.

reduce workability loss to near zero, a target behavior for printability. Fig. 21 shows the flowability evolution for compositions with an ANC contents of 0.5% C.M. and 0.8% C.M (each with a calcium aluminate cement content of 5.0% C.M. and 37 °C water), when mixed for 28 and 43 min after the addition of water. The composition with ANC content of 0.5% C.M. is Mix 5, and is detailed in Table 2. For both the 0.5% and 0.8% ANC compositions, the portion of the paste (including fibers) that was mixed for an additional 15 min shows matching flowability evolution to those portions only mixed for 28 min, indicating near zero workability loss under continued shear agitation.

Near zero workability loss allows the material to exhibit the

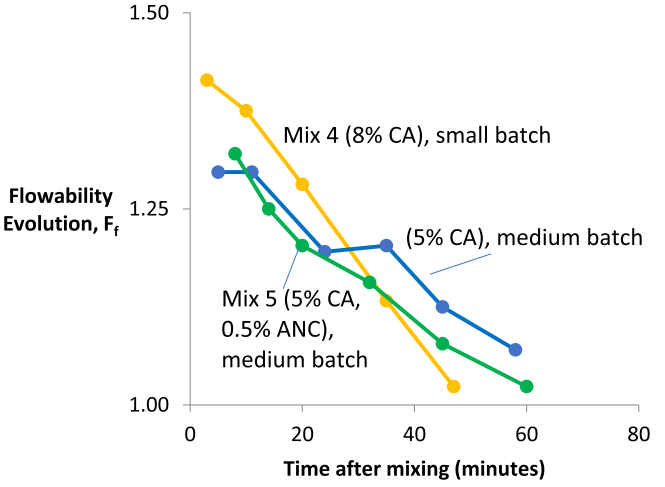

Fig. 19. The flowability of the Mix 4 composition can be approximated in a larger batch size when the calcium aluminate cement composition is reduced to 5.0% C.M and with the addition of 0.5% Attapulgite nanoclay. Both medium batches included here use 37 °C water, while the small batch uses room temperature water.

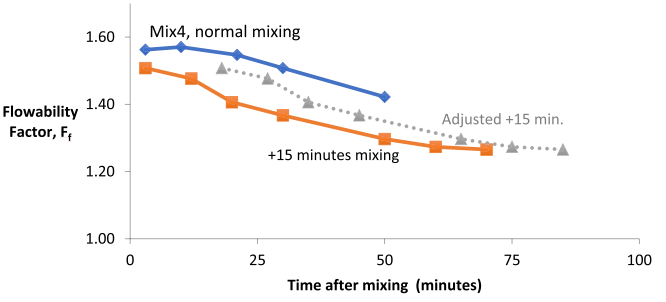

Fig. 20. Mix 4 showed significant workability loss, indicated by the lower flowability factor values at similar time intervals, under an additional 15 min of shear agitation. The discrepancy between the top curve and the dotted curve illustrates the contribution of additional mixing, as opposed to simply time, to workability loss for this particular composition.

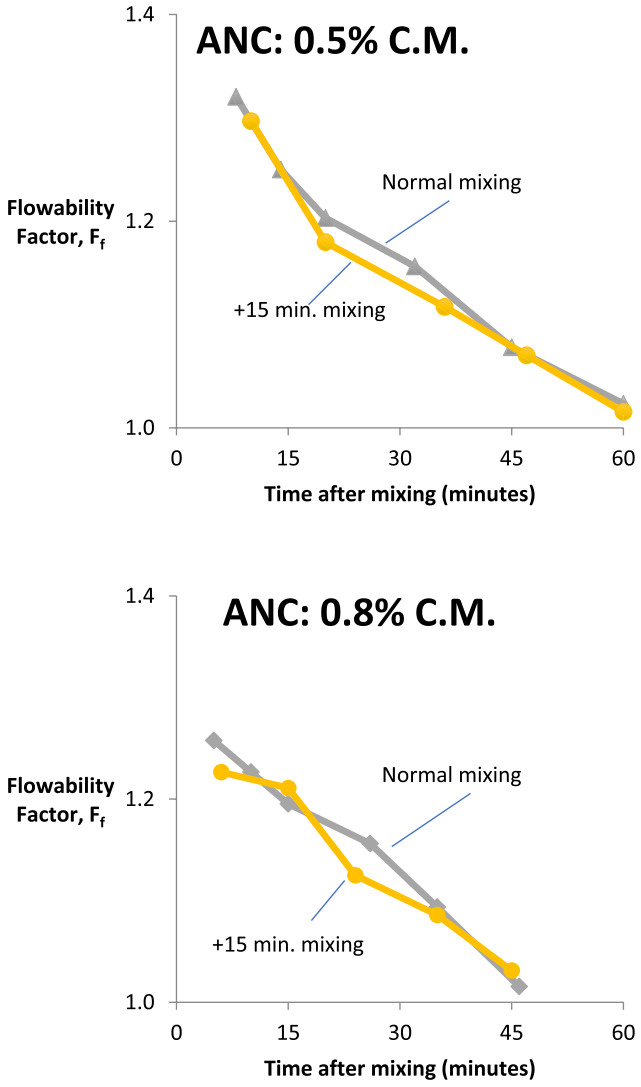

Fig. 21. Compositions with calcium aluminate cement content of 5.0% C., 37 °C water, and ANC content of (a) 0.5% C.M. and (b) 0.8% C.M., show minimal workability loss under an additional 15 min of shear agitation (mixing); minimal workability loss under these conditions indicate a highly consistent printable material.

"harden on command" type behavior described in Fig. 3 as being a target for printability.

3.6. Scaled printing approximation

Due to the minimal workability loss, appropriate flowability evolution, and robust strain-hardening behavior (Fig. 22) exhibited by the Mix 5 composition, it was used for a large-scale printing approximation (Fig. 23).

The Mix 5 composition exhibited great extrudability and immediate buildability as well as sustained printability over a period of time. The material showed clay-like workability with shear thinning behavior and rapid rebuilding that allowed both extrusion and buildability with minimal deformation of layers under the weight of subsequent layers. Several stacks of 6–9 layers, and 30 cm in length, were produced. The filament produced was approximately 1 cm thick (height) and 4 cm wide. The rate of deposition was intentionally slowed to simulate the longer time between deposition passes that would be characteristic of larger print sizes.

4. Conclusions

The influences of several compositional ingredients on fresh state flowability evolution were reported. Calcium aluminate cement, HPMC, microsilica, ground silica, purified and exfoliated attapulgite nanoclay, and water content were used to manipulate fresh state rheological behavior. HPMC can be used to manipulate initial flowability, but is not effective in manipulating rate of hardening. Dosage of CA is seen to have a large effect on rate of hardening, as well as on initial flowability. Substituting MS and GS for a fractional portion of silica sand content also increases rate of hardening, while maintaining initial flowability. Small amounts of ANC reduced time to hardening via reduced workability, but showed only a slight effect on rate of hardening. For compositional additions or substitutions, water content may need to be adjusted to allow proper mixing and fiber dispersion, which can both affect mechanical performance.

A printable cementitious material design paradigm, based on minimizing workability loss under continued shear agitation, was proposed and used to guide printable cementitious composite development. Purified and exfoliated attapulgite nanoclay was seen to minimize workability loss under relevant processing conditions. The workability loss mitigation provided by ANC was negated when increased rate of hardening caused by excessive CA content dominated. A limited CA content in combination with ANC is recommended to maintain low workability loss for robust printability.

Batch size and temperature of the water content added during processing were seen to be two processing parameters that have a significant effect on fresh state rheological properties. Water temperature can also be used to intentionally manipulate fresh state properties. It is recommended that both batch size and water

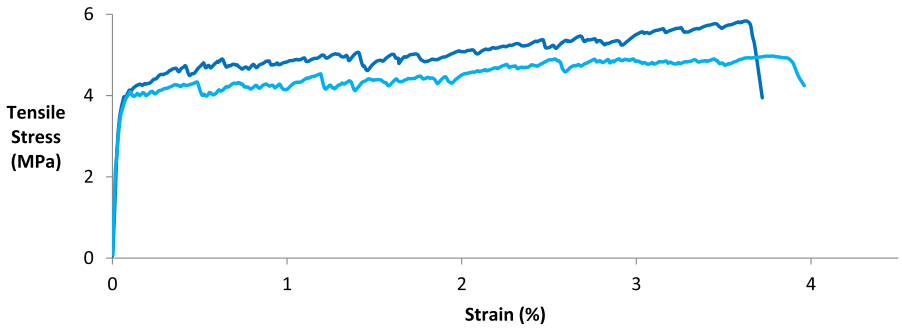

Fig. 22. Representative stress-strain curves illustrating the tensile performance of the Mix 5 composition, showing robust strain-hardening behavior.

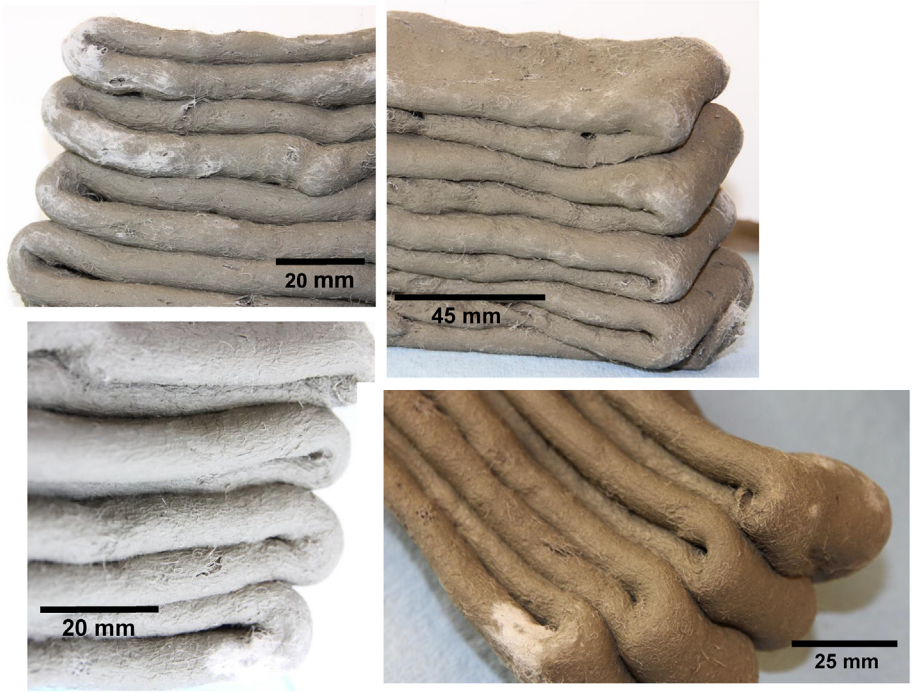

Fig. 23. Large-scale printing approximations produced with the Mix 5 composition, showing a combination of extrudability, buildability and appropriate hardening/early strength behavior.

temperature be monitored and controlled for consistent, predictable printing performance.

Compositions exhibiting both extrudability and buildability in the fresh state and interlayer bonding and robust strain-hardening in the cured state were systematically designed and demonstrated on a variety of scales. The mesoscale material structuring produced by the printing process was seen to improve mechanical performance in direct tension due to fiber alignment, without negatively affecting compressive strength.

The early stage properties of the Mix 5 composition indicate a promising printable composition. Robust tensile strain-hardening behavior of this composition has been confirmed, which will contribute to durability and resilience of the material and structural members produced with it. This printable ECC material exhibited tensile strain capacity of ~4.0%, and tensile strength approaching 6 MPa. Compressive strength for this composition is gained quickly, conservatively measured to reach 30 MPa within 6 days. Extrudability and immediate buildability was observed during a demonstration of an approximated printing process.

The effects of compositional ingredients and processing parameters demonstrated in this paper can be used to manipulate the early stage behaviors as needed for specific applications, processing equipment, and project scale.

Funding

This work was supported by the University of Michigan through the MCubed program.

Acknowledgements

The authors thank Bob Spence and Jan Pantolin for instrument maintenance and technical support, Jeff Plott, Albert Shih, Greg Keolian, and Evgueni Filipov for discussions and support, Headwaters Resources (Monroe, MI, USA) for donation of fly ash materials, Elkem for donation of Microsilica, and the University of Michigan MCubed cross-disciplinary research funding program for supporting and encouraging innovative, multi-disciplinary collaborative research.

Appendix. ASupplementary data

Supplementary data related to this article can be found at https://doi.org/10.1016/j.cemconcomp.2018.03.017.

APPENDIX I. Materials

Presented here is additional information regarding the materials used in the cementitious composites reported in this study. The information presented in this appendix was provided by the materials' respective manufacturers/suppliers.

Table I.1
Compositional of Lafarge Type I Portland Cement, Alpena, MI plant

Compositional Component	Content (%)
SiO_2	19.6
Al_2O_3	4.6
Fe_2O_3	3.0
CaO	63.5
MgO	2.6
SO_3	2.6
Loss on ignition	2.6
Insoluble residue	0.32
Free lime	1.4
CO_2	1.7
Limestone	4.3
$CaCO_3$ in limestone	87.0

Table I.2
Class F fly ash chemical composition as provided by Headwaters Resources, Monroe, Michigan Plant

Compositional Component	Content (%)
Silicon Dioxide (SiO_2)	39.77
Aluminum Oxide (Al_2O_3)	20.00
Iron Oxide (Fe_2O_3)	9.74
Sum (SiO_2+Al_2O_3+Fe_2O_3)	69.51
Sulfur Trioxide (SO_3)	1.95
Calcium Oxide (CaO)	18.88
Magnesium Oxide (MgO)	3.67
Sodium Oxide (Na_2O)	1.23
Potassium Oxide (K_2O)	1.20
Sodium Oxide Equivalent (Na_2O+0.658K_2O)	2.02
Moisture	0.18
Loss on Ignition	0.86
Available Alkalis, as Na_2Oe	1.14

Table I.3
Chemical composition of Elkem Microsilica (Silica Fume) Grade 955 (undensified)

Compositional Component	Content (%)
SiO_2	95.5 (min)
C_{free}^{**}	1.0 (max)
Fe_2O_3	0.3 (max)
Al_2O_3	1.0 (max)
CaO	0.4 (max)
MgO	0.5 (max)
K_2O	1.0 (max)
Na_2O	0.4 (max)
H_2O^*	1.0 (max)

*when packed.
**C in SiC not counted.

References

[1] S. Lim, R.A. Buswell, T.T. Le, S.A. Austin, A.G.F. Gibb, T. Thorpe, Developments in construction-scale additive manufacturing processes, Autom. ConStruct. 21 (January 2012) 262–268.
[2] N. Labonnote, A. Rønnquist, B. Manum, P. Rüther, Additive construction: state-of-the-art, challenges and opportunities, Autom. ConStruct. 72 (2016) 347–366.
[3] P. Wu, J. Wang, X. Wang, A critical review of the use of 3-D printing in the construction industry, Autom. ConStruct. 68 (2016) 21–31.
[4] F. Bos, R. Wolfs, Z. Ahmed, T. Salet, Additive manufacturing of concrete in construction: potentials and challenges of 3D concrete printing, Virtual Phys. Prototyp. 11 (3) (2016).
[5] Y.W.D. Tay, B. Panda, S.C. Paul, N.A.N. Mohamed, M.J. Tan, K.F. Leong, 3D printing trends in building and construction industry: a review, Virtual Phys. Prototyp. 12 (3) (2017).
[6] S.J. Keating, J.C. Leland, L. Cai, N. Oxman, Toward site-specific and self-sufficient robotic fabrication on architectural scales, Sci. Robot. 2 (26 April 2017).
[7] A. Warszawski, R. Navon, Implementation of robotics is building: current status and future prospects, J. Constr. Eng. Manag. J. 124 (1) (1998) 31–41.
[8] D. Hwang, B. Khoshnevis, An innovative construction process-contour crafting (CC), in: Proceedings of the 22nd International Symposium on Automation and Robotics in Construction ISARC 2005, Ferrara, Italy, September, 2005.
[9] R.A. Buswell, R.C. Soar, A.G.F. Gibb, A. Thorpe, Freeform construction: Mega-scale rapid manufacturing for construction, Autom. ConStruct. 16 (2) (2007) 224–231.
[10] T.S. Rushing, G. Al-Chaar, B.A. Eick, J. Burroughs, J. Shannon, L. Barna, M. Case, Investigation of concrete mixtures for additive construction, Rapid Prototyp. J. 23 (1) (2017) 74–80.
[11] T.T. Le, S.A. Austin, S. Lim, R.A. Buswell, A.G.F. Gibb, T. Thorpe, Mix design and fresh properties for high-performance printing concrete, Mater. Struct. 45 (8) (2012) 1221.
[12] A. Kazemian, X. Yuan, E. Cochran, B. Khoshnevis, Cementitious materials for construction-scale 3D printing: Laboratory testing of fresh printing mixture, Construct. Build. Mater. 145 (1 August 2017) 639–647.
[13] M. Hambach, D. Volkmer, Properties of 3D-printed fiber-reinforced Portland cement paste, Cement Concr. Compos. 79 (May 2017) 62–70.
[14] S. Metsa-Kortelainen, T. Vehmas, J. Lagerbom, A. Kronlof, R. Mahlberg, H. Heinonen, Biomimetic Building of 3D Printed Tailored Structures, VTT Technical Research Centre of Finland, Research Report VTT-r-00669–14 MIMECOMP Commissioned by Tekes (Public), March 2014.
[15] V.C. Li, On engineered cementitious composites (ECC): a review of the material and its applications, J. Adv. Concr. Technol. 1 (3) (November 2003) 215–230.
[16] H. Kong, S.G. Bike, V.C. Li, Constitutive rheological control to develop a self-consolidating engineered cementitious composite reinforced with hydrophilic poly(vinyl alcohol) fibers, Cement Concr. Compos. 25 (3) (April 2003) 333–341.
[17] Y.Y. Kim, H. Kong, V.C. Li, Design of engineered cementitious composite suitable for wet-mixture shotcreting, ACI Mater. J. 100 (6) (Nov 2003) 511–518.
[18] Q. Zhang, V.C. Li, Development of durable spray-applied fire-resistive engineered cementitious composites (SFR-ECC), Cement Concr. Compos. 60 (2015) 10–16.
[19] Z. Quanji, Thixotropic Behavior of Cement-based Materials: Effect of Clay and Cement Types, Iowa State University, 2010. Graduate Theses and Dissertations, Paper 11724.
[20] Ö. Kirca, Temperature Effect on Calcium Aluminate Cement Based Composite Binders, the Graduate School of Natural and Applied Sciences of Middle East Technical University, July 2006. Doctoral Thesis.
[21] G. Abbas, S. Irawan, K.R. Memon, S. Kumar, A.A.I. Elrayah, Hydroxyproylmethylcellulose as a primary viscosifying agent in cement slurry at high temperature, Int. J. Automot. Mech. Eng. 8 (July-December 2013) 1218–1225.
[22] ThM. Salem, Electrical conductivity and rheological properties of ordinary Portland cement–silica fume and calcium hydroxide–silica fume pastes, Cement Concr. Res. 32 (9) (September 2002) 1473–1481.
[23] A.R. Hariharan, A.S. Santhi, M. Ganesh, Study on strength development of high strength concrete containing fly ash and silica fume, Int. J. Eng. Sci. Technol. 3 (4) (Apr 2011).
[24] S. Kawashima, M. Chaouche, D.J. Corr, S.P. Shah, Rate of thixotropic rebuilding of cement pastes modified with highly purified attapulgite clays, Cement Concr. Res. 53 (2013) 112–118.
[25] S. Kawashima, M. Chaouche, D.J. Corr, S.P. Shah, Influence of purified attapulgite clays on the adhesive properties of cement pastes as measured by the tack test, Cement Concr. Compos. 48 (2014) 35–41.
[26] JSCE, Recommendations for Design and Construction of High Performance Fiber Reinforced Cement Composites with Multiple Fine Cracks (HPFRCC), Japan Society of Civil Engineers, March 2008. Concrete Engineering Series 82.